Two-dimensional wetting transition in a corrugated potential

1998 J. Phys. A: Math. Gen. 31 L549

(http://iopscience.iop.org/0305-4470/31/32/001)

J. Phys. A: Math. Gen. **31** (1998) L549–L557. Printed in the UK PII: S0305-4470(98)94126-9

LETTER TO THE EDITOR

Two-dimensional wetting transition in a corrugated potential

Theodore W Burkhardt

Department of Physics, Temple University, Philadelphia, PA 19122, USA

Received 28 May 1998, in final form 23 June 1998

Abstract. A simple model for the wetting or depinning transition of a two-dimensional solid-on-solid (SOS) interface in a short-range periodic pinning potential which alternates between attraction and infinite repulsion is analysed exactly. The interface is specified by transverse displacement variables x_i which vary *continuously* in the interval $x_{\min} < x_i < \infty$, and the stretching energy is proportional to $\sum_i |x_{i+1} - x_i|$. Both the semi-infinite and infinite geometries $x_{\min} = 0, -\infty$ are considered. For the most part the wetting transition in the continuum model is similar to the transition in restricted SOS models with corrugated potentials, in which the x_i are restricted to integers and $x_{i+1} - x_i$ to $\pm 1, 0$, but there are some qualitative differences in the phase diagrams involving re-entrant behaviour.

The wetting transition in the semi-infinite two-dimensional Ising model with a short-range interface pinning force at the boundary was first studied in detail by Abraham [1] in 1980. At the wetting temperature T_W the second temperature derivative of the interface free energy is discontinuous, and the characteristic lengths $\xi_\perp$, $\xi_\parallel$ of interface fluctuations diverge as $(T_W - T)^{-1}$, $(T_W - T)^{-2}$, respectively, as T approaches T_W from below. Following publication of [1], many authors [2–10] pointed out that simply soluble solid-on-solid (SOS) models, in which the position of the interface is specified by transverse displacement variables x_i, with $i = 0, \pm 1, \pm 2, \ldots, \pm\infty$, exhibit depinning transitions in the same universality class. This is true both of discrete SOS models, in which the x_i are restricted to integers, and models in which the x_i vary continuously.

Recently Nechaev and Zhang [11] studied the wetting transition in an SOS model with a 'corrugated' pinning potential that alternates between attraction and repulsion. Swain and Parry [12] extended their work. Corrugated pinning potentials are of interest in connection with the more complicated case of walls with random roughness [11–16].

Roughly speaking, an interface bound near a wall unbinds, as the temperature is raised, when the entropic repulsion due to the hard wall exceeds the attraction due to the pinning potential. There is no such repulsion in the case of an interface in the infinite geometry subject to a purely attractive pinning force, and the interface remains bound at all temperatures [2–10]. On the other hand, corrugated potentials that alternate between attraction and repulsion do give rise to entropic repulsion in the infinite geometry. Nechaev and Zhang [11] showed that with corrugated potentials there are wetting transitions with the same universal characteristics described above in both the the semi-infinite and infinite geometries, even when the average interaction is repulsive.

The results of Nechaev and Zhang [11] and Swain and Parry [12] were obtained for restricted solid on solid (RSOS) models, in which the transverse displacements x_i of the

0305-4470/98/320549+09$19.50

interface are restricted to integers and $x_{i+1}-x_i$ to $\pm 1, 0$. In this paper an analogous system with *continuously* varying x_i (CSOS model) is considered. The CSOS Hamiltonian is

$$\mathcal{H} = J \sum_{\text{all } i} |x_{i+1} - x_i| + \sum_{\text{odd } i} U_1(x_i) + \sum_{\text{even } i} U_2(x_i) \tag{1}$$

where $x_{\min} < x_i < \infty$, with $x_{\min} = 0$ and $x_{\min} = -\infty$ for the semi-infinite and infinite geometries. The three sums in equation (1) represent the stretching energy of the interface and the pinning potential energy for odd and even i. The CSOS interface is less rigid than the RSOS interface, both at low and high temperatures, since $x_{i+1} - x_i$ may take both very small and very large values. The depinning transition of the noncorrugated CSOS model with $U_1(x) = U_2(x)$ is considered in [2]. The purpose of this letter is to point out some qualitative differences in the phase diagrams of the corrugated CSOS and RSOS models involving re-entrant behaviour. In both corrugated models the wetting transition has the same universal features described in the introductory paragraph.

The interface free energy of the CSOS model of equation (1) is determined by the largest eigenvalue λ of the transfer matrix or kernel. The eigenvalue λ and eigenfunction $\psi(x)$ satisfy the integral equation

$$\lambda\psi(x) = \int_{x_{\min}}^{\infty} \mathrm{d}y \, \exp[-K|x-y| - V_2(y)] \int_{x_{\min}}^{\infty} \mathrm{d}z \, \exp[-K|y-z| - V_1(z)]\psi(z) \tag{2}$$

where $K = J/k_BT$, and $V(x) = U(x)/k_BT$. With the identity $(-\mathrm{d}^2/\mathrm{d}x^2 + K^2)\exp(-K|x-y|) = 2K\delta(x-y)$, equation (2) may be converted to the integro-differential equation

$$\left(-\frac{\mathrm{d}^2}{\mathrm{d}x^2} + K^2\right)\psi(x) = \frac{2K}{\lambda}\exp[-V_2(x)] \int_{x_{\min}}^{\infty} \mathrm{d}z \exp[-K|x-z| - V_1(z)]\psi(z) \; . \tag{3}$$

For a *piecewise-constant* potential $V_2(x)$, such as a rectangular well or barrier, a second application of the identity yields the fourth-order differential equation

$$\left(-\frac{\mathrm{d}^2}{\mathrm{d}x^2} + K^2\right)^2 \psi(x) = \frac{(2K)^2}{\lambda}\exp[-V_1(x) - V_2(x)]\psi(x) \; . \tag{4}$$

We now consider the semi-infinite geometry $x > x_{\min} = 0$ and the corrugated potential

$$U_1(x) = \begin{cases} \infty & x < 0 \\ -U_0 & 0 < x < R_1 \\ 0 & x > R_1 \end{cases} \qquad U_2(x) = \begin{cases} \infty & x < R_2 \\ 0 & x > R_2 \end{cases} \tag{5}$$

with $R_2 > R_1$, which is alternately attractive and infinitely repulsive. For $R_2 > R_1$ the stretching and the pinning potential energies in equation (1) compete, i.e. are minimized by different interface configurations, and the average potential $\frac{1}{2}(U_1 + U_2)$ is repulsive.

With the corrugated potential (5) it is simple to calculate λ and $\psi(x)$. Since the right-hand side of equation (3) vanishes for $x < R_2$ and the right-hand side of equation (4) equals $(2K)^2\lambda^{-1}\psi(x)$ for $x > R_2$, the bound eigenfunction has the form

$$\psi(x) = \begin{cases} \alpha \mathrm{e}^{Kx} + \beta \mathrm{e}^{-Kx} & 0 < x < R_2 \\ \mu_1 \mathrm{e}^{-P_1 x} + \mu_2 \mathrm{e}^{-P_2 x} & x > R_2 \end{cases} \tag{6}$$

where $P_2 > P_1 > 0$ and

$$-P_1^2 + K^2 = P_2^2 - K^2 = \frac{2K}{\sqrt{\lambda}}. \tag{7}$$

Equation (2) implies $\psi'(0)/\psi(0) = K$ and the continuity of $\psi(x)$ and $\psi'(x)$ at $x = R_2$. Thus $\beta = 0$, $\mu_1 = (K+P_2)(P_2-P_1)^{-1}\mathrm{e}^{(K+P_1)R_2}\alpha$, and $\mu_2 = (K+P_1)(P_1-P_2)^{-1}\mathrm{e}^{(K+P_2)R_2}\alpha$. Substituting (6) with these β, μ_1, and μ_2 into (3) leads to a further requirement,

$$(\mathrm{e}^{V_0}-1)(\mathrm{e}^{2KR_1}-1) - [4K(K+P_1)(P_2-K)^{-1}(P_2-P_1)^{-1}-1]\mathrm{e}^{2KR_2}-1 = 0 \tag{8}$$

where $V_0 = U_0/k_BT$, for a consistent solution. Equations (7) and (8) determine the decay constants P_1 and P_2 in (6). The criticality condition for the wetting or depinning transition

$$(\mathrm{e}^{V_0}-1)(\mathrm{e}^{2KR_1}-1) - (2\sqrt{2}+3)\mathrm{e}^{2KR_2}-1 = 0 \tag{9}$$

follows from equation (8) in the limit $P_1 = (2K^2 - P_2^2)^{1/2} \to 0$.

The structure of the bound interface is examined in more detail in the appendix, where the probability density for the displacement variable x_i is calculated.

We now turn to the CSOS model in the infinite geometry, i.e. $x_{\min} = -\infty$ in equations (2) and (3), and consider the corrugated pinning potential

$$U_1(x) = \begin{cases} -U_0 & |x| < R_1 \\ 0 & |x| > R_1 \end{cases} \qquad U_2(x) = \begin{cases} \infty & |x| < R_2 \\ 0 & |x| > R_2 \end{cases} \tag{10}$$

with $R_2 > R_1$. The bound-state eigenfunction $\psi(x)$ satisfying (2)–(4) is an even function of x and for $x > 0$ is given by (6) with $\alpha = \beta$. Using the continuity of $\psi(x)$ and of $\psi'(x)$ at $x = R_2$ and substituting (6) into (3), one finds that P_1 and P_2 satisfy

$$\begin{aligned}(\mathrm{e}^{V_0}-1)(2KR_1 + \sinh 2KR_1) + 2KR_2 + \sinh 2KR_2 - 4K(K^2-P_1^2)^{-1}(P_2-P_1)^{-1} \\ \times[K(P_1+P_2)\sinh 2KR_2 + (K^2+P_1P_2)(\cosh 2KR_2 - 1) + 2P_1P_2] = 0\end{aligned} \tag{11}$$

which implies the criticality condition

$$(\mathrm{e}^{V_0}-1)(2KR_1 + \sinh 2KR_1) + 2KR_2 - 3\sinh 2KR_2 - 2\sqrt{2}(\cosh 2KR_2 - 1). \tag{12}$$

For comparison we also consider an analogous RSOS model, in which x_i are restricted to integers and $x_{i+1} - x_i$ to $\pm 1, 0$. In the semi-infinite geometry a corrugated potential similar to the CSOS potential with $R_2 > R_1$ is imposed by restricting the allowed x_i to integers $x_i \geqslant 0$ for odd i and to integers $x_i \geqslant 1$ for even i. The energy of an interface configuration is defined as j times the number of nonvanishing $|x_{i+1} - x_i|$ minus u times the number of vanishing x_i with i odd. This is a special case of more general models considered in [11, 12]. For even n the partition function $Z(x, n)$ of an interface with ends at x, n and x_0, n_0 satisfies

$$Z(1, n+2) = [1 + (\mathrm{e}^{v}+1)t^2]Z(1, n) + 2tZ(2, n) + t^2Z(3, n) \tag{13}$$

$$Z(2, n+2) = 2tZ(1, n) + (1+2t^2)Z(2, n) + 2tZ(3, n) + t^2Z(4, n) \tag{14}$$

$$\begin{aligned}Z(x, n+2) = {} & t^2Z(x-2, n) + 2tZ(x-1, n) + (1+2t^2)Z(x, n) \\ & +2tZ(x+1, n) + t^2Z(x+2, n) \qquad x = 3, 4, \ldots, \infty\end{aligned} \tag{15}$$

where $t = \mathrm{e}^{-k}$, $k = j/k_BT$, $v = u/k_BT$.

Difference equations that determine the eigenvectors $\psi(x)$ and eigenvalues λ of the transfer matrix follow from the substitution $Z(x, n) \to \psi(x)\lambda^{n/2}$ in equations (13)–(15). One finds a single-bound eigenvector

$$\psi(x) = \alpha[\mathrm{e}^{-p_1x} - (-1)^x\mathrm{e}^{-p_2x}] \qquad x = 1, 2, \ldots, \infty \tag{16}$$

$$\cosh p_2 = \cosh p_1 + \mathrm{e}^{k} = \tfrac{1}{2}(\lambda^{1/2}+1)\mathrm{e}^{k} \tag{17}$$

$$\mathrm{e}^{v} = 1 + \mathrm{e}^{p_1+p_2}\ . \tag{18}$$

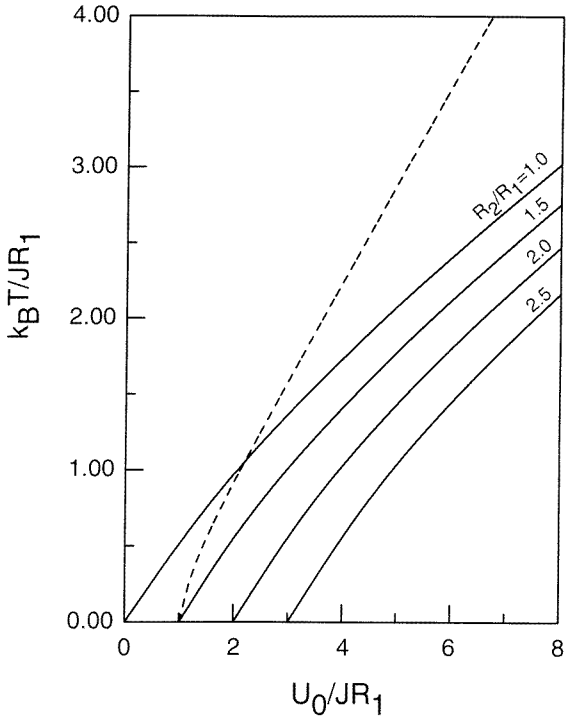

Figure 1. Critical line (9) for the semi-infinite CSOS model (full curves) and the corresponding RSOS result (19) in the variables k_BT/j, u/j (broken line).

In the limit $p_1 \to 0$ equations (17) and (18) yield the criticality condition

$$e^v = e^k[1 + 2e^{-k} + (1 + 2e^{-k})^{1/2}]. \tag{19}$$

Finally we consider the infinite-space version of this RSOS model. The energy of an interface configuration is defined as above, but now the allowed x_i are $0, \pm 1, \pm 2, \ldots, \pm\infty$ for odd i and $\pm 1, \pm 2, \ldots, \pm\infty$ for even i. The partition function satisfies equations (14) and (15), but an extra term $e^v t^2 Z(-1, n)$ must be included on the right-hand side of (13). Since the bound state has even parity, $\psi(x)$ is again given by (16) and (17), but e^v on the left-hand side of (18) and (19) is replaced by $2e^v$.

The critical line (9) for the semi-infinite CSOS model (1) with the corrugated pinning potential (5) is shown in the variables $k_BT/JR_1, U_0/JR_1$ in figure 1 for several values of R_2/R_1. The broken curve is the corresponding RSOS critical line (19) in the variables k_BT/j, u/j.

The areas below and above a given critical line in figure 1 correspond to the pinned and depinned phases, respectively. The transition temperature increases monotonically as the strength U_0 of the pinning potential increases and as the range R_2 of the repulsive barrier decreases, as expected. At $T = 0$ the CSOS critical line intersects the horizontal axis at $U_0 = 2J(R_2 - R_1)$. This intercept corresponds to a transition in the ground state of the system. The lowest-energy interface is straight, unbound, and infinitely degenerate for $U_0 < 2J(R_2 - R_1)$ but bound for $U_0 > 2J(R_2 - R_1)$, with x_i zig-zagging between R_1 and R_2 for odd and even i, respectively.

The lowest energy RSOS interface is also straight and unbound for $u < 2j$ and bound with a zig-zag form for $u > 2j$. In contrast to the CSOS case, the broken RSOS critical

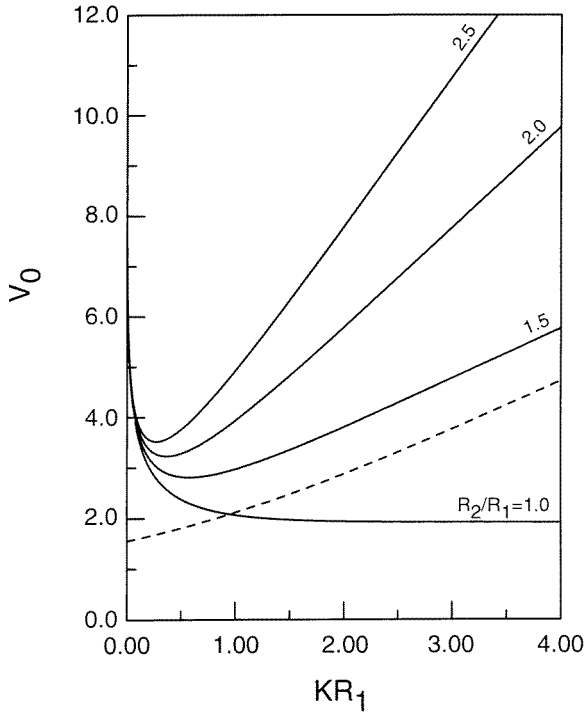

Figure 2. Critical line (9) for the semi-infinite CSOS model (full curves) and the corresponding RSOS result (19) in the variables v, k (broken line).

line in figure 1 does not intersect the horizontal axis at $u = 2j$, where the ground state transition takes place, but at $u = j$. The 're-entrance' of the critical line at $T = 0$, pointed out by Nechaev and Zhang [11], has its origin in the discrete RSOS energy spectrum. The interface is bound for $j < u < 2j$ at very low temperatures, despite the unbound, infinitely degenerate ground state, because the lowest-energy excitations of the straight interface cost less energy ($2j - u$ instead of j) if the straight interface is at $x_i = 1$ instead of $x_i = 2, 3, \ldots$.

In figure 2 the CSOS and RSOS critical lines of figure 1 are replotted in terms of the variables V_0, KR_1 and v, k of equations (9) and (19), respectively. The areas above and below a given critical line correspond to the pinned and depinned phases, respectively.

The CSOS critical lines in figure 2 have a double-valued, re-entrant form. For $R_2 > R_1$ a bound interface eventually unbinds as KR_1 increases at constant V_0 and it becomes too taut to conform to the pinning potential. A bound interface also eventually unbinds as KR_1 decreases at constant V_0 and the interface fluctuations increase, due to entropic repulsion from the hard wall.

In contrast to the CSOS critical lines in figure 2, the broken RSOS critical line is monotonic. A bound RSOS interface does not unbind as k decreases at constant v, since the constraint $x_{i+1} - x_i = \pm 1, 0$ severely limits the entropic repulsion.

We now turn from the semi-infinite to the infinite geometry. The critical line (12) for the infinite CSOS interface model (1) with the corrugated pinning potential (10) is shown in the variables $k_BT/JR_1, U_0/JR_1$ in figure 3 for several values of R_2/R_1. The broken curve is the corresponding RSOS critical line (equation (19) with $e^v \to 2e^v$) in the variables k_BT/j, u/j. The low-temperature behaviour in figures 1 and 3 is very similar, and the intercepts of

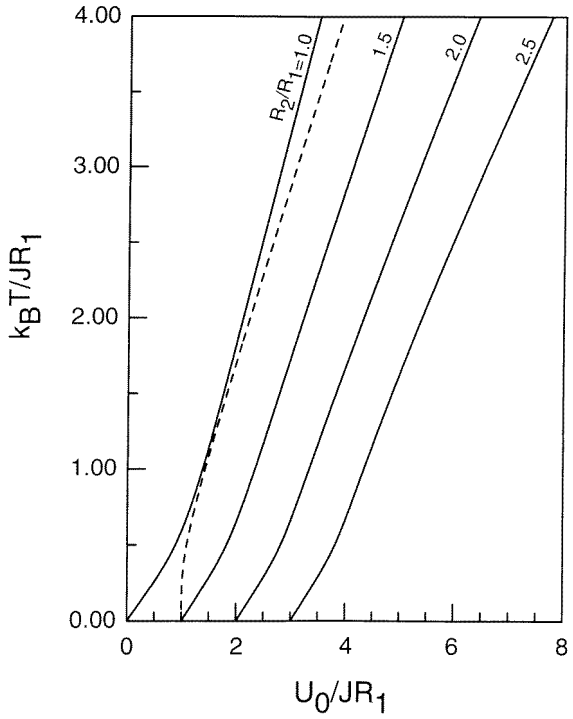

Figure 3. Critical line (12) for the infinite CSOS model (full curves) and the corresponding RSOS result ((19) with $e^v \to 2e^v$) in the variables k_BT/j, u/j (broken curve).

the horizontal axis at $T = 0$ are the same. At low temperatures it does not matter whether there is an impenetrable wall at $x_i = 0$, i odd or not, because the interface fluctuations are small, and the repulsive part of the corrugated potential pushes the interface out beyond $x_i = 0$. For the same reason as in the semi-infinite geometry, the critical line of the infinite RSOS model is re-entrant at $T = 0$. The critical line intersects the $T = 0$ axis at $u = j$, while the ground-state transition is at $u = 2j$. The curves in figure 1 rise less steeply than in figure 3 due to the greater entropy of repulsion in the semi-infinite geometry.

In figure 4 the CSOS and RSOS critical lines of figure 3 for the infinite geometry are replotted in terms of the variables V_0, KR_1 and v, k of equations (12) and (19) with $e^v \to 2e^v$, respectively. In contrast to the semi-infinite CSOS results shown in figure 2, V_0 is finite in the limit $KR_1 \to 0$ and increases monotonically with KR_1. Without the extra entropic repulsion due to the impenetrable wall at $x_i = 0$ for i odd, a bound interface does not unbind as KR_1 is reduced at constant V_0.

In the depinning transitions of the corrugated CSOS and RSOS models in both the semi-infinite and infinite geometries, the critical exponents are the same as for ordinary critical wetting (see the first paragraph). This is because the decay constants P_1 and p_1 of the bound CSOS and RSOS interfaces, defined by (6) and (16), respectively, vanish linearly as the critical line is approached along any nontangential straight line.

In summary we have found two main differences between the transitions of the CSOS and RSOS models with corrugated potentials.

(1) In contrast to the CSOS model, the critical lines of both the semi-infinite and infinite RSOS models are re-entrant at $T = 0$. In figures 1 and 3 the RSOS critical lines intersect

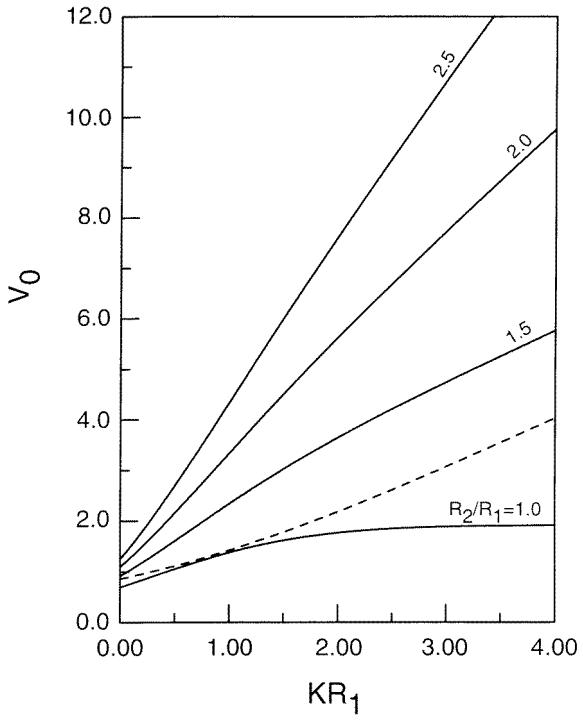

Figure 4. Critical line (12) for the infinite CSOS model (full curves) and the corresponding RSOS result ((19) with $e^v \to 2e^v$) in the variables v, k (broken line).

the $T = 0$ axis at $u = j$, whereas the ground-state transition takes place $u = 2j$. This has its origin in the discrete energy spectrum of the RSOS model. For $j < u < 2j$ the interface is bound at low but nonzero temperatures, despite a straight, infinitely degenerate, unbound ground state, because low-energy excitations cost less energy if the straight interface is at $x_i = 1$ rather than $x_i = 2, 3 \ldots$.

(2) In contrast to the RSOS model, the critical line of the semi-infinite CSOS model in the variables V_0, KR_1 (see figure 2) has a re-entrant form. For very large KR_1 the interface is too taut to conform to the corrugated potential and is unbound. As KR_1 is reduced at constant V_0, the interface first binds and then, as the entropic repulsion increases, unbinds. Neither the infinite CSOS model nor the semi-infinite and infinite RSOS models undergo this second transition.

Appendix

For a bound CSOS interface the probability densities $P_1(x_i)$, $P_2(x_i)$ for the displacement variable x_i, with i odd and even, respectively, are given by

$$P_1(x) = c_1\psi(x)^2 e^{-V_1(x)} \qquad P_2(x) = c_2\phi(x)^2 e^{-V_2(x)}. \tag{A1}$$

Here c_1 and c_2 are normalization constants, chosen so that $\int_{x_{\min}}^{\infty} P(x)\,dx = 1$, $\psi(x)$ is given in equation (6), and $\phi(x)$ is proportional to the integral on the right-hand side of (3). From equations (3), (6), and (7)

$$\phi(x) = \mu_1 e^{-P_1 x} - \mu_2 e^{-P_2 x} \qquad x > R_2. \tag{A2}$$

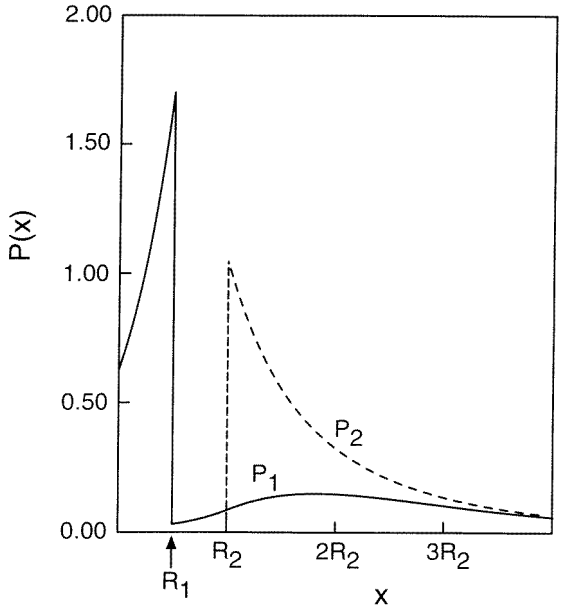

Figure A1. Probability densities $P_1(x)$ (full curve) and $P_2(x)$ (broken curve) for the bound interface of the semi-infinite CSOS model with $R_2 = 2R_1$, $KR_1 = \frac{1}{2}$, and $V_0 = 4$.

With $\psi(x)$ and $\phi(x)$ normalized as in (6) and (A2), $c_1 = c_2$ in (A1).

The probability densities $P_1(x)$ and $P_2(x)$ for the bound interface of the semi-infinite CSOS model with $R_2 = 2R_1$, $KR_1 = \frac{1}{2}$, and $V_0 = 4$ are shown in figure A1. Recall that R_1 and R_2, defined in equation (5), are the ranges of the attractive and infinitely repulsive parts of the corrugated potential. The function $P_1(x)$ (full curve) is strongly enhanced for $0 < x < R_1$ and discontinuous at $x = R_1$, due to the factor $e^{-V_1(x)}$ in equation (A1). The other function $P_2(x)$ (broken curve) vanishes identically for $x < R_2$, due to the factor $e^{-V_2(x)}$ in (A1). In its ground state the interface zig-zags back and forth between the values $x_i = R_1$ and R_2 for odd and even i, respectively. Note that the probability densities $P_1(x)$ and $P_2(x)$, which, of course, include thermal fluctuations, have peaks at these same values. As x increases past R_2, the corrugated potential influences the interface increasingly less, and the two curves in figure A1 approach each other. Both $P_1(x)$ and $P_2(x)$ decay asymptotically as ae^{-2P_1x} for large x, with the same amplitude a.

References

[1] Abraham D B 1980 *Phys. Rev. Lett.* **44** 1165
[2] Burkhardt T W 1981 *J. Phys. A: Math. Gen.* **14** L6
[3] Chalker T 1981 *J. Phys. A: Math. Gen.* **14** 2431
[4] Chui T and Weeks J D 1981 *Phys. Rev.* B **23** 2438
[5] van Leeuwen J M J and Hilhorst H 1981 *Physica* **107A** 319
[6] Kroll D M 1981 *Z. Phys.* **41** 345
[7] Vallade M and Lajzerowicz J 1981 *J. Physique* **42** 1505
[8] Fisher M E 1984 *J. Stat. Phys.* **34** 667
[9] Privman V and Svrakic N M 1988 *J. Stat. Phys.* **51** 1111
[10] Burkhardt T W 1989 *Phys. Rev.* B **40** 6987
[11] Nechaev S and Zhang Y-C 1995 *Phys. Rev. Lett.* **74** 1815

[12] Swain P S and Parry A O 1997 *J. Phys. A: Math. Gen.* **30** 4597
[13] Lipowsky R and Fisher M E 1986 *Phys. Rev. Lett.* **56** 472
[14] Forgacs G, Lipowsky R and Nieuwenhuizen Th M 1991 *Phase Transitions and Critical Phenomena* vol 14, ed C Domb and J L Lebowitz (New York: Academic)
[15] Derrida B, Hakim V and Vannimeus J 1992 *J. Stat. Phys.* **66** 1189
[16] Giugliarelli G and Stella A L 1997 *Physica* **239A** 467